

1 **A comparison of annual layer thickness model estimates with observational measurements using**
2 **the Berkner Island ice core, Antarctica**

3 A. Massam^{*,1,2}, S. Sneed³, G. Lee^{1,4}, R. Tuckwell¹, R. Mulvaney¹, P.A. Mayewski³, P. Whitehouse²

4 *Corresponding author: ashsm73@bas.ac.uk

5 ¹British Antarctic Survey, High Cross, Cambridge, CB3 0ET, UK

6 ²Department of Geography, Durham University, South Road, Durham, DH1 3LE, UK

7 ³Climate Change Institute, University of Maine, 133 Sawyer Research Building, Orono, ME

8 ⁴School of Environmental Sciences, University of East Anglia, Norwich Research Park, Norwich, NR4
9 7TJ, UK 04469-5741

10 **Abstract**

11 A model to estimate the annual layer thickness of deposited snowfall at a deep ice core site,
12 compacted by vertical strain with respect to depth, is assessed using ultra-high resolution laboratory
13 analytical techniques. A recently established technique of high-resolution direct chemical analysis of
14 ice, using ultra-violet laser ablation inductively-coupled plasma mass spectrometry (UV LA ICP-MS)
15 has been applied to ice from the Berkner Island ice core, and compared with results from lower-
16 resolution techniques conducted on parallel sections of ice. The results from both techniques have
17 been analysed in order to assess the capability of each technique to recover seasonal cycles from
18 deep Antarctic ice. Results do not agree with the annual layer thickness estimates from the age-
19 depth model for individual samples less than one metre long as the model cannot reconstruct the
20 natural variability present in annual accumulation. However, when compared with sections over 4 m
21 long, the deviation between the modelled and observational layer thicknesses is minimised to within
22 two standard deviations. This confirms that the model is capable of successfully estimating mean
23 annual layer thicknesses around analysed sections. Furthermore, our results confirm that the LA
24 ICP-MS technique can reliably recover seasonal chemical profiles beyond standard analytical
25 resolution.

26 Keywords: ultra-high resolution; mass spectrometry; age-depth model; chemistry; glaciology

27

28 **Introduction**

29 The deposition of snow across Antarctica results in a record spanning millennia which is capable of
30 recording seasonal cycles of several different climatic proxies, revealing past climatic conditions on
31 local, regional and global scales, on both short- and long-term timescales. Preservation of temporal
32 variations in stable water isotopes and chemistry as the deposited snow turns to ice creates an
33 isotope-chemistry series that can provide seasonal to glacial/interglacial reconstructions of past
34 climate (Dansgaard 1953, 1964).

35 Unreactive gases trapped within the ice matrix offer continuous records of atmospheric conditions
36 on a global scale due to rapid rates of atmospheric mixing. In order to reconstruct large-scale
37 climatic events on an inter-hemispheric scale, climate proxies from multiple sources must be
38 integrated and tied to a single chronology, which requires a continuous, high-resolution record.
39 Accurate synchronisation of ice core records with climate proxy records from marine, polar and
40 terrestrial sites gives the best view of global climate responses during glacial/interglacial periods,
41 and high-resolution profiles are vital to the full interpretation of the timing and characteristics of
42 underlying mechanisms and to understanding the relationship between the Polar Regions and the
43 rest of the Earth.

44 The dating of deep Antarctic ice cores still relies primarily on modelled accumulation derived from
45 seasonal cycles in the stable water isotopes and chemistry. Therefore, improvements to existing
46 chronologies depend on further developments of the analytical techniques. The low mean annual
47 accumulation characterizing much of Antarctica makes it difficult to obtain sub-annually resolved
48 proxy records in ice cores beyond certain depths. Therefore, the construction of Antarctic ice-core
49 chronologies – and the subsequent interpretation of palaeoclimate records – typically relies on
50 glaciological modelling techniques that are constrained using observational data, e.g. known-age
51 horizons preserved in the ice or chemical records. Increasing the resolution of palaeoclimate
52 records improves the information that can feed into climate or chronological models. The models

53 applied to ice-core profiles rely on the resolution of the stable water isotope profile as well as a
54 number of glaciological assumptions on ice-sheet stability and they therefore have larger age-
55 uncertainty compared to annual-layer counted ice-core chronologies.

56 As water isotopes tend to diffuse in ice and the seasonal cycles may be lost, improvements to
57 analytical resolution have been progressing following two main approaches, continuous and discrete
58 trace-element analysis. A direct, continuous method (continuous flow analysis – CFA) takes
59 measurements continuously along the length of the ice core. CFA methods are less labour-intensive,
60 although they usually result in the destruction of the ice core by melting. Continuous melting of an
61 ice section coupled with the *in situ* analysis of trace-chemical species by ICP-MS and UV/visible
62 spectroscopy improves the resolution of continuous records and achieves a spatial resolution of ~10
63 mm (Sigg et al. 1994, Rothlisberger et al. 2000). A great advantage of CFA systems is their relatively
64 low contamination levels, ensured by removing the meltwater produced by the outermost part of
65 the ice core. A disadvantage of CFA systems is the dispersion in the melting and liquid transport that
66 limits the sub-annual resolution of deep Antarctic ice cores and consequently, the degree to which
67 information available on long timescales can be accurately synchronised with other climate proxy
68 archives.

69 Developments to direct trace-element analysis improve the depth-resolution by the application of
70 ultra-violet laser sampling coupled with an ICP-MS. For some time, LA ICP-MS has been applied to
71 geological samples in order to optimise the resolution and accuracy of trace-element analysis in
72 geochemical contexts (Arrowsmith 1987, Bea et al. 1996). More recently, this technique in ultra-
73 high resolution direct trace-element analysis has been independently developed in ice-core
74 laboratories (Reinhardt et al. 2001, Müller et al. 2011, Sneed et al. 2015). Previous studies have
75 demonstrated that the ultra-violet LA ICP-MS apparatus and calibration technique developed at the
76 WM Keck Laser Ice Facility at the Climate Change Institute (University of Maine) yields profiles that
77 are similar in shape and trend of the ice-core profile to those produced using CFA analysis, but at

78 orders of magnitude higher resolution (Sneed et al. 2015). Correlation of LA ICP-MS results with
79 existing chemical records on alpine ice-core chemistry profiles confirms the reproducibility of the
80 results (Sneed et al. 2015). Further to this, LA ICP-MS can be utilized as a basis of comparison for
81 previous studies; a recent study dramatically increased the resolution of the record comprising the
82 end of the Younger Dryas and the onset of the Holocene as preserved in the GISP2 ice core
83 (Mayewski et al. 2014). This ultra-high resolution record offered a novel view of abrupt climate
84 change over this period and suggested a decrease in storm frequency and an increase in the length
85 of the Arctic summer season at this transition (Mayewski et al. 2014). Most recently, LA ICP-MS has
86 been applied to West Antarctic ice originating from the last glacial period at Siple Dome-A.
87 Successful analysis of sub-seasonal profiles demonstrated the variability in the annual layer thickness
88 measurements that had not been identified earlier in glaciological models or ice core chemistry
89 (Haines et al. 2016).

90 In addition to increased resolution of climate records, major advantages of the LA ICP-MS technique
91 include the rapid analysis time and the fact that the ultra-violet laser results in negligible ice loss,
92 allowing repeated analyses to be carried out (Müller et al. 2011). In repeating the analysis,
93 individual line scans can be used to measure single- and multi-element arrays, increase the spatial
94 resolution available, and provide an alternative approach to acquiring ultra-high resolution profiles
95 of climatic proxies in ice cores.

96 An alternative discrete high-resolution technique, developed by R. Mulvaney and E. Wolff (pers.
97 comm) at the British Antarctic Survey, cuts samples at a higher resolution than standard discrete
98 techniques of ~10 mm by employing a microtome device to shave the ice sample at a sub-millimetre
99 resolution (Thomas et al. 2009). Seasonal cycles in chemistry recovered in glacial ice from the North
100 Greenland Ice Core Project (NGRIP) ice core allowed an absolute measurement of annual layer
101 thickness and insight into the phasing of chemical signals and characteristics of the DO 8 event at
102 *circa* 38 ka BP at 2 mm depth-resolution (Thomas et al. 2009). A full geochemical profile outlined

103 the dominant and recessive mechanisms for the duration of the climatic transition into DO 8 at sub-
104 annual resolution. The method, though effective for high-resolution analysis on deep ice, is labour-
105 intensive and it is difficult to cover more than small sections of an ice core. Improvements to the ion
106 chromatography system at the British Antarctic Survey – principally a new Dionex 4000 IC system –
107 allow a reduced sample volume and therefore improve the spatial resolution of each measurement.

108 Despite these advances in direct ice-core analysis, LA ICP-MS is yet to be employed on ice originating
109 from the Weddell Sea, Antarctica, where traditional discrete and CFA methods fail to recover
110 seasonal chemical cycles at great depths. The aim of this study is to compare the different analytical
111 techniques, and then use the results to test the accuracy of the modelling of the annual layer
112 thickness of the Berkner Island ice core. The Berkner Island ice core was drilled over three field
113 seasons 2003-2006 (Mulvaney et al. 2007), reaching the ice sheet base at a depth of 948 m, at the
114 south dome of the island, which is embedded within the Ronne and Filchner ice shelves in the
115 Weddell Sea, Antarctica. In this study, we reconstruct annual layer thickness from the stable water
116 isotope profiles and glaciological modelling and, following a study to assess the reliability of the
117 records, we assess these model estimates with the observational annual layer thickness
118 measurements obtained by LA ICP-MS.

119 **Methodology**

120 High-resolution analysis, completed on parallel sections of ice from three depth ranges along the
121 Berkner Island ice core, was achieved by indirect and direct trace-element methods. For comparison
122 and confirmation of the record obtained by LA ICP-MS on Antarctic frozen samples, discrete
123 sampling has been completed on parallel sections of ice to obtain a second geochemical profile.
124 Where the annual layer thickness is estimated to be greater than 20 mm, the discrete samples were
125 not cut using the microtome technique, but instead a band saw was used for which an associated ice
126 loss is calculated. The ion profiles generated by each method have been compared by identifying
127 annual peaks in each profile and calculating the mean annual layer thickness for each section. For

128 assistance in the identification of annual layer peaks, a long section of CFA data is presented for the
129 Berkner Island ice core at a depth where sub-annual resolution is still attainable by this lower-
130 resolution technique.

131 Successively, comparison of annual layer thickness measurements with the annual layer thickness
132 estimated from the model is the final assessment in this work. The methodology for the annual
133 layer thickness model is included in the supplementary material, accompanied with a list of the
134 parameters and known-age horizons used in the estimation of annual layer thickness at Berkner
135 Island.

136 *Continuous Flow Analysis*

137 A full ice core can be continuously melted in core sections with the dimensions of 30 x 30 mm, with
138 only the inner part of the ice section measured to eliminate the risk of contamination. The
139 remainder of the ice section melted runs off the melt-head as waste. Analysis of the Berkner Island
140 ice core by CFA was completed at BAS, on a system that is capable of measuring a full ion profile
141 among other chemical species, at a continuous rate with a maximum resolution of 10 mm.

142 *LA ICP-MS and Discrete Sample Details*

143 The ice core retrieved from Berkner Island was selected for this study for its low mean annual
144 accumulation at the surface, with an overall thickness of 948 m. Present-day mean annual
145 accumulation at the core site is 0.185 m yr^{-1} in water equivalent, with an age-depth profile reaching
146 the last interglacial period. As a result, the annual layer thickness model estimates that the depth at
147 which thinned annual layers are beyond the standard laboratory resolution of $\sim 10 \text{ mm}$ is $\sim 560 \text{ m}$.
148 This leaves 40% of the total ice core profile beyond the reach of sub-annual profiles using standard
149 methods.

150 Parallel sticks of ice, cut from the archived ice core material, have been analysed by two methods
151 including high and ultra-high resolution measurements. Sticks of ice were cut from the inner section

152 of the ice core to avoid potential contamination by the drilling fluid residue on the exterior of the ice
153 core. Sticks of ice were placed in plastic lay-flat bags with the ice core bag number and top of the
154 core section clearly indicated.

155 *LA ICP-MS*

156 The analysis of Berkner Island ice using LA ICP-MS was completed at the WM Keck Laser Ice Facility,
157 at the Climate Change Institute (CCI), University of Maine. The laser-ablated ICP-MS methodology is
158 largely described in Sneed et al. (2015) and only a brief summary of the key features is features is
159 mentioned here. Profiles were acquired using the Sayre CellTM cryocell, developed at CCI, which is
160 capable of holding up to one metre of ice at 248 K and has a small volume (~20 cm³) open-design
161 ablation chamber. The cryocell system is positioned underneath a New Wave UP-213 laser,
162 connected to a Thermo Element 2 ICP-MS with Teflon tubing (Sneed et al. 2015).

163 Prior to analysis, the ice sample was cleaned by removing the outer millimetre of ice using a ceramic
164 scraper to limit the contamination risk. The ice is held in the cryocell whilst the gas flow was purged
165 for two minutes in order to remove impurities in the system. Individual line scans, measured using a
166 laser spot size of 100 µm in diameter, yield the ultra-high spatial resolution of LA profiles. LA ICP-MS
167 profiles are continuous for 40 mm; once finished, the ice is automatically moved to begin the next 40
168 mm segment, starting at the end of the previous ablation pass. Adjacent line scans, used for multi-
169 element analysis, are separated by 200 µm to prevent overlapping scans. Sampling resolution is 121
170 µm sample⁻¹; this resolution is dependent on the laser spot diameter, firing rate, scan speed and the
171 ICP-MS sampling rate (Sneed et al. 2015).

172 Ice samples, up to 200 mm in length, were analysed for sodium (Na), which has been shown to have
173 a clear annual cycle (Sommer et al. 2000). The LA ICP-MS generates results available in counts per
174 second (cps). The relative intensity of element concentrations in cps were converted to

175 concentrations ($\mu\text{g/L}$) using calibration curves constructed from liquid samples and lasing frozen
176 standard reference material (Sneed et al. 2015).

177 A dual-cyclonic spray chamber with entrance ports for liquid samples and laser aerosols is fitted to
178 the ICP-MS system. A low-flow nebuliser ($20 \mu\text{L min}^{-1}$ from Elemental Scientific) aims to reduce the
179 amount of liquid aspirated and to enable higher gas flow in the laser ablation chamber. This
180 facilitates daily calibration of the ICP-MS, which is completed using a combination of liquid standards
181 and frozen reference materials in a two-step process outlined by Sneed et al. (2015). To ensure
182 accurate results using the Sayre Cell™ cryocell, the base of the open cell must have an airtight seal
183 with the ice sample. Soundness of the seal is tested in two ways: (i) a flowmeter built into the
184 cryocell system, and (ii) the ICP-MS is tuned with the ice in place so that a small leak would be
185 observable in the ice chemistry signal (Sneed et al. 2015).

186 *Discrete Samples*

187 For the deepest sections investigated by LA ICP-MS, we obtained discrete samples from a parallel cut
188 of the same ice core, to be measured in solution mode. This method has been used successfully to
189 analyse the warming transition of Dansgaard-Oeschger 8 (DO8), at *circa* 38kyr in Greenland ice
190 (Thomas et al. 2009).

191 Unlike the ice sampled by the other techniques in this study, sections of ice for the discrete method
192 were limited to 80 mm in length. The reason for this was to limit the bending moment exerted on
193 the stick of ice as it passed under the blade whilst being held in the microtome vice system. The
194 depth ranges of discretely-cut samples are included in table I.

195 Prior to cutting the discrete samples, any dust or residue was removed from the instruments by
196 cleaning the microtome blade and mantle using isopropanol. A pre-frozen section of ultra-high
197 purity (UHP) water was passed under the blade to clean it thoroughly; after this process, five

198 samples of UHP water were collected for use as a background standard for the cold room procedure
199 during the chemical analysis.

200 A clean microtome blade removed the outer millimetre of ice in order to avoid contamination from
201 the outer layers. The ice was then placed in the mantle of the microtome and passed under the
202 blade. The mantle automatically raises 40 μm with every forward stroke so the exact sample size
203 can be determined by the number of times the ice has passed under the blade.

204 *Lower Resolution Discrete Sampling*

205 A lower-resolution discrete sampling method was employed on sections of ice for which annual layer
206 thickness is estimated to be greater than 20 mm. For these sections, the high-resolution microtome
207 technique would not be necessary and instead 5 mm discrete samples were cut using a band saw
208 and measured using the same method as samples obtained from the microtome device. An
209 associated ice loss of a millimetre was accounted for in the depth profile, as calculated by the width
210 of the band saw blade.

211 For all discrete samples, a full ion profile was obtained in sterile conditions by ion chromatography
212 (IC). In order to prevent contamination during the discrete sampling process, protective clothing and
213 powder-free nitrile gloves were worn throughout both the sampling and analysis procedures. The
214 ice sample was only handled with pre-cleaned tongs and the outer millimetre of the ice sample was
215 scraped away using a scalpel or microtome blade to remove any contaminants from the surface of
216 the sample. Ion profiles were measured on a Dionex IC 4000 ion chromatography system in a class-
217 100 clean room, which has less than 100 particles of $0.5 \mu\text{m m}^{-3}$.

218 **Results**

219 We begin by presenting the estimated age and layer thickness of the analysed samples, as derived
220 using the glaciological model. Subsequent sections contain the LA ICP-MS and discrete sampling
221 results, respectively. Annual cycles are identified in the IC and LA ICP-MS records based on the

222 prominence of the Na and Mg peaks from the baseline, and the return of the peak to the baseline
223 between the seasons. Peaks that do not return to the baseline are characterised as discrete events
224 within one annual cycle.

225 *Model Estimates*

226 Specific sampled depths were chosen based on the estimated period of original deposition, as
227 interpreted from the isotopic record (fig. 1), the modelled annual layer thickness (equation S1-S3),
228 and ultimately the condition of the archive material at BAS (presented in table I).

229 *CFA Results*

230 As a method of comparison, and to aid the analysis of annual layer identification, a four-metre
231 section of the Berkner Island ice core at 447 m, analysed by CFA, is presented with the correlating
232 dielectric profiling (DEP) data (fig. 2). The section shows a mean annual layer thickness of ~57 mm,
233 and highlights the variable annual layer thickness and values of Na.

234 *LA ICP-MS on Mid-Holocene Ice from 5.5 ka BP (454 – 459 m)*

235 Fig. 3 shows the sections of ice analysed by LA ICP-MS originating from the mid-Holocene period.
236 Three sections were taken from the depth range 454 – 459 m, where the model predicts the annual
237 layer thickness to be ~57 mm (table I). Results are presented on semi-logarithmic plots. Red dashed
238 lines delineate peaks that could represent either an annual or sub-seasonal deposition in Na. It is
239 not confirmed if these peaks in Na are definitive annual layers or discrete events within an annual
240 cycle, with a mean annual layer thickness much thinner than the estimated values and the annual
241 layer thickness observed in the DEP and CFA Na profiles at 447-451 m.

242 *LA ICP-MS on Glacial Ice from 27.1 – 27.7 ka BP (694 – 697 m)*

243 Over the second depth range of 694 – 697 m, the mean annual layer thickness is estimated by
244 disregarding sections of ice where the chemical signal is not resolvable (~19 – 38 mm and ~50 – 70

245 mm). In these sections in fig. 4, a black dashed line marks where the annual signal is not discernible.
246 An increase in the seasonal periodicity per sampled section of ice, as determined by the seasonal
247 fluctuations in Na, is due to the compaction of annual layers. In fig. 4c, a drop in concentration at 40
248 mm is likely due to the recommencement of a line scan.

249 *LA ICP-MS on Glacial Ice from 29.7 – 31.2 ka BP (702 – 707 m)*

250 Similar to the sections of ice analysed from 694 – 697 m, there is a drop in concentration values at
251 40 mm in fig. 5a, and 80 mm in fig. 5c, due to the recommencement of line scans. Additionally, as
252 with the observed layer thickness estimations from 694 – 697 m, observed layer thickness has been
253 estimated only for sections of ice where a seasonal signal is resolvable in the ice. Layer thickness is
254 counted between ~10 – 25 mm and ~45 – 60 mm in fig. 5a, yielding an average annual layer
255 thickness of 3.1 mm. Across the ice sections analysed between 702 and 707 m, the chemical signal
256 appears to be a smoothed signal where annual layers are no longer resolvable either in the ice-core
257 record or through the analytical technique. Where identifiable in these profiles, the frequency of
258 the peaks appear to increase from ~3 mm in fig. 5b to 5-6 mm in fig. 5c.

259 Initial observations on the geochemical profiles confirm that fluctuations in the Na⁺ signal are visible
260 in the Berkner Island ice-core record. These layers do not show a clear seasonal pattern in many
261 places, with variations in strength, thickness and signature common throughout the profiles. This is
262 most visible between the Holocene sections at 454 – 459 m and the late glacial sections at 695 – 697
263 m where the number of layers over a common depth range increases by up to a factor of 10.

264 Focussing on the LA ICP-MS profiles between the depths of 454 – 459 m it is not possible to identify
265 a uniform annual layer thickness, despite a relatively stable isotopic record for this depth range (fig.
266 1a, 3a – c). The layers identifiable in these sections range in thickness between 5 and 30 mm,
267 compared with the 39 mm estimated in the annual layer thickness model.

268 Within the profiles analysed from a depth 694 m and deeper, sections of ice appear to have little
269 seasonality in the analysed profiles (fig. 4a and 5c). These results raise the following questions
270 regarding the reliability of LA ICP-MS at greater depths: firstly, is the method capable of obtaining
271 sub-annual cycles in ice originating from the last glacial period, preserved in the Berkner Island ice
272 core? Secondly, has the chemical signal diffused at these depths, leading to a smoothed record in
273 the ice? The answers to these questions will partly be addressed by determining the repeatability of
274 the ultra-high resolution results using the alternative, established methods.

275 In the deepest analysed sections of the ice core the observed mean annual layer thickness doubles
276 between 695 m and 704 m, suggesting a significant increase in annual accumulation at the time of
277 original deposition. This is contrary to what has been predicted by the model that is unable to
278 identify natural variability not preserved in the stable water isotope profile.

279 The results presented have been obtained using both lower- and high-resolution discrete sampling
280 methods. Results are presented as semi logarithmic plots of chemical profiles against the sample
281 length, mm.

282 *Discrete Sampling on Mid-Holocene Ice from 5.5 ka BP (454 – 459 m)*

283 Discrete samples were cut roughly at a 5 mm spatial resolution on sections of ice parallel to ice
284 analysed by LA ICP-MS. In addition, the dataset has been expanded by sampling an additional 100 –
285 150 mm of ice per metre of ice in each depth range. Fig. 6 displays the results from this study, and
286 the expanded profiles for sections of ice sampled from 455 – 459 m, with red dashed lines indicating
287 the point at which a peak is visible. An immediate observation of the three expanded profiles is that
288 seasonality appears smoothed throughout each profile, with a variable annual layer thickness of 50-
289 70 mm that agrees with the CFA profiles and annual layer thickness model. Additional chemistry and
290 the DEP datasets for the corresponding depths have been included for a thorough comparison of the
291 between the LA ICP-MS Na and the lower-resolution datasets (fig. 7-8). The LA ICP-MS Na signal is

292 presented in two ways: (i) the log of the original high-resolution dataset; (ii) a logarithmic profile of
293 the smoothed LA ICP-MS Na to the lower resolution used in the discrete sampling. Sub-seasonal
294 discrete events are visible in the sodium and chloride profiles but are not identifiable in the non-sea
295 salt Sulphur (nss-S) and DEP datasets. Annual layers are delineated with grey bands in each figure, in
296 comparison to the red dashed lines in previous plots where chemical peaks could have been
297 interpreted as an annual signal.

298 *Discrete Sampling on Glacial Ice from 29.7 – 31.2 ka BP (702 – 707 m)*

299 A microtome blade was used to discretely cut samples for two sections of ice, originating from the
300 last glacial period, at a spatial resolution of 320 – 480 μm . The results of these analyses are
301 displayed in fig. 9-10, against the LA ICP-MS results. The IC profiles are displayed as semi logarithmic
302 plots of trace-element sodium, (Na^+), magnesium (Mg^{2+}), and calcium (Ca^{2+}) against sampled depth
303 (mm). Only a cation profile is available for ice at 703.2 – 703.22 m due to low sampling volume,
304 meaning there is only a sulphate signal available at 706.3 – 706.38 m in this depth range.

305 Additional annual layers are identified in the lower-resolution profile, suggesting that the loss of an
306 annual signal during the LA ICP-MS analysis is due to the capability of the technique and that the
307 seasonal record of the Berkner Island ice core is resolvable and preserved.

308 **Discussion**

309 The methods employed in this study have all used a sample resolution where seasonal variability
310 should be visible in the resulting profile based on the estimated annual layer thicknesses at each
311 analysed depth. As a result, the detection of annual layers is dependent on three factors: (i) the
312 preservation of a seasonal cycle in the ice-core record, (ii) the reliability of the method to extract the
313 seasonality, and (iii) whether the sampling resolution was sufficient. The following section will
314 discuss the feasibility of each analytical approach to obtain a seasonal profile on the ice used as part
315 of this study.

316 Analysis of ice at depths 454 – 459 m using the lower-resolution discrete technique was not
317 successful in replicating the trends seen in the high-resolution profile due to the high sampling
318 volume required (fig. 7-8). This led us to investigate the small-scale variations resolved in the high-
319 resolution analysis that suggest the LA ICP-MS technique was able to measure sub-annual discrete
320 events within an annual layer. In addition to this sub-seasonal variability, the profile shows the
321 changes in annual accumulation in short timeframes. The Holocene period shows no consensus of a
322 mean annual accumulation rate that is consistent over the timeframe analysed, suggesting a highly
323 variable annual accumulation. Both of these unresolved can be answered by comparison of the
324 high-resolution datasets with longer timeseries of annual layers from the Berkner Island ice core.
325 Wagenbach et al. (1994) presented a high-resolution profile for the upper depths of ice at two
326 domes (north and south) on Berkner Island. The annually resolved profiles demonstrated significant
327 variability in annual layer thickness over a depth range of 11 m; similarly, within this study, CFA and
328 the corresponding DEP profile in the deep Berkner Island record also replicates natural variability
329 (fig. 2). Results show a mean annual layer thickness that matches the modelled estimate for the
330 total depth range, but the measured profile demonstrates great variability over a couple of metres.

331 This study has assessed the preservation of annual layers in ice originating from the last glacial
332 period by comparison with lower-resolution techniques. Good correlation can be seen between LA
333 ICP-MS profiles and profiles derived using lower-resolution techniques on ice from the last glacial
334 period, as well as comparison of each sampling technique with the modelled estimates (fig. 9-10;
335 table I). The trend, magnitude and frequency of Na cycles suggests that annual layers are visible and
336 that these methods can be applied to deep Antarctic ice cores with confidence that the technique is
337 capable of a sub-annual resolution where annual layers are at least as small as 3 mm.

338 In the deeper section, continuous seasonal profiles are not always visible in the record despite the
339 annual layer thickness estimated to be greater than the resolution of all the techniques employed.
340 This implies a potential loss of signal within the ice core record, resulting in a smoothed profile with

341 limited seasonal fluctuations. However, this loss of seasonality in the record is not repeated in the
342 lower-resolution discretely cut ice core profile at 702 – 707 m (fig. 9-10), suggesting the annual
343 record is still resolvable at this depth. In glacial ice, annual layer thickness appeared to increase
344 dramatically; this increase in annual layer thickness from ~3 mm at 704 m to ~6 mm at 706 m
345 indicates significant natural variability not previously identified through modelling techniques.

346 *Annual Layer Visibility in the LA ICP-MS Record*

347 The cycles visible in the laser-ablated profiles follow the pattern expected of ice core annual layers.
348 The greatest annual layer thicknesses are visible in the upper depths of the ice core, with the
349 number of seasonal cycles visible increasing with depth due to the compaction of annual layers in
350 the ice core. The patterns that emerge as the analysed depth increases indicate that the ultra-high
351 resolution method at shallower depths results in a “noisy” signal. The low sampling volume required
352 makes the LA ICP-MS profiles more sensitive to small scale variations; as the layer thickness of the
353 cycles decrease with depth, the number of small-scale variations also decreases, suggesting that the
354 main cause for this “noise” in the signal is the analytical resolution.

355 The seasonal layers visible in the Berkner Island ice, retrieved at a depth in the ice sheet previously
356 unattainable by standard laboratory resolution, confirm that our results are in line with other studies
357 suggesting that LA ICP-MS is a valuable technique for high-resolution ice core analysis (Müller et al.
358 2011, Mayewski et al. 2014, Sneed et al. 2015). Since the initial development of LA ICP-MS on frozen
359 samples, the technique has been established through successful application to Greenland and alpine
360 ice. Most notably, LA ICP-MS demonstrated a clear sub-annual view of abrupt climate events
361 including the onset of the Holocene in the GISP2 record as well as the assessment of the capability to
362 identify sea ice and dust markers in the GRIP ice core record (Reinhardt et al. 2001, Mayewski et al.
363 2014). In particular, the ultra-high resolution records that can be produced using LA ICP-MS have
364 the potential to enhance the information available to constrain age-depth models; the profiles
365 presented as part of this study show that the method is capable of inferring climatic variability not

366 recorded in the stable isotopic history of the ice core such as rapid changes in mean annual
367 accumulation.

368 In addition to the ultra-high spatial resolution achieved when using LA ICP-MS on frozen samples,
369 the contribution of LA ICP-MS to ice-core analyses is significant. The rapid analysis time, permitted
370 by the balance between the laser spot diameter and high spatial resolution, means it is possible to
371 measure a 40 mm profile in several minutes. Furthermore, the methodology and implementation of
372 an ultra-violet laser is non-destructive to the frozen samples unlike both discretely-cut and IR LA ICP-
373 MS. These features of ultra-violet LA ICP-MS add support to the recommendation that this
374 technique should be applied to frozen samples where possible in order to improve the resolution of
375 an ice core profile, and the subsequent chronology and palaeoclimate analysis.

376 *Discrete Sampling*

377 The lower-resolution sampling technique used to analyse the sections of ice originating from the
378 Holocene does not reproduce results obtained by laser ablation. Seasonal variations detected by the
379 high-resolution LA ICP-MS results are beyond the 5 mm sampling resolution of the lower-resolution
380 technique. Similarities in the broad shape profile of the lower-resolution profiles suggest a
381 smoothed record that is comparable to the shape and trends in the high-resolution LA ICP-MS
382 record. These results agree with the comparison study on the Colle Gnifetti ice core, which found
383 that lower-resolution CFA was unable to detect seasonal variability but showed a profile resembling
384 a smoothed version of the ones acquired by LA ICP-MS (Sneed et al. 2015).

385 In ice originating from the last glacial period, a higher and variable spatial resolution of 320 – 480 μm
386 was necessary. The results presented in fig. 9-10 correlate well with the corresponding ultra-high
387 resolution records, and help confirm the potential of LA ICP-MS on Antarctic ice from the last glacial.
388 Annual layers identified throughout each analysed profile correspond well, though discrepancies are

389 apparent between the discretely sampled and laser-ablated profiles, with more annual layers
390 identifiable in the lower-resolution profile.

391 *Assessment of the Annual Layer Thickness Model*

392 As part of this study, a model was used primarily to estimate the annual layer thickness along the ice
393 core to assist the initial sampling observations (see the supplementary data to this article). The
394 confirmation that seasonal profiles are visible in the glacial ice permits a second comparison study;
395 the observational data with the modelled layer thickness estimates. By comparing these two
396 profiles, the model can be independently validated and give insight into the empirical relationships
397 that contribute to age-depth determinations.

398 Table I outlines the depths (m, to the nearest integer) that have been sampled and analysed by LA
399 ICP-MS and the discrete sampling techniques, the observed annual layer thickness (if available), and
400 the modelled annual layer thickness estimate and standard deviation (2σ , mm). The results of the
401 ultra-high resolution analysis, in comparison with the modelled annual layer thickness
402 approximations, demonstrate that the model is successful in estimating the annual layer thickness
403 along the ice core at each depth section except for the depth range 704 – 707 m.

404 The Holocene record produced by LA ICP-MS does not agree with the modelled estimates,
405 suggesting a highly variable accumulation profile that cannot be accurately modelled to account for
406 small-scale variations in accumulation variability over several years. Looking at a broader view, the
407 mean annual layer thickness over the four metres analysed by CFA is 57.0 ± 8.8 mm, and $51.75 \pm$
408 3.51 mm for the discretely-measured profiles. Both mean annual layer thickness values are within
409 the confidence interval of the mean modelled estimate of 59.75 ± 6.9 mm.

410 The small uncertainties attached to the measured and estimated annual layer thicknesses allow
411 corroboration between the high and low sampling resolutions and the model estimates on ice
412 originating from the last glacial period. Estimates agree to within a millimetre, but not the

413 prescribed error margin for ice analysed at a depth of 694-704 m. Similar to the Holocene sections,
414 for the full 10 m section of glacial ice analysed, the mean annual layer thickness measured by LA ICP-
415 MS is 3.4 ± 0.2 mm, which corroborates with the mean modelled annual layer thickness estimate of
416 3.0 ± 0.2 mm.

417 The inter annual mean annual layer thickness measurements agree with the modelled estimates for
418 each depth section analysed, suggesting that the model is able to estimate annual layer thickness for
419 sections of the ice-core on a metre resolution or greater, but cannot accurately reconstruct natural,
420 local variability in the accumulation profile. This is unsurprising as the resolution of this model is
421 0.55 m, based on the resolution of the stable water isotope data in the accumulation reconstruction
422 (eq. S1).

423 At 704 m, the layer thickness observations deviate from the estimated profile due to an increase in
424 annual layer thickness despite continued compaction along the ice core and no evidence in the
425 isotopic record to suggest a deviation from the ice-core physics of strain and layer compaction. The
426 age estimate at 706 m (~ 32 ka BP) coincides with a large increase in stable nitrogen isotopes ($\delta^{15}\text{N}$)
427 identified in the gas-phase of Berkner Island (Mani 2010). From 37 ka BP, a large, positive excursion
428 in $\delta^{15}\text{N}$ begins and does not return to start-values for ~ 10 ka. One suggestion for this excursion in
429 $\delta^{15}\text{N}$ records is a rapid and significant increase in the accumulation rate that increased the firn
430 diffusive height, and the gravitational fractionation. This accumulation increase would have been
431 rapid in order to leave little-to-no trace in the isotopic record. It is highly probable that the deepest
432 section of ice analysed by LA ICP-MS corresponds to this signature preserved in the gas-phase
433 record, and that the observed increase in annual layer thickness within this section strengthens the
434 hypothesis of a rapid increase in annual accumulation. However, the employment of further analysis
435 by ultra-high resolution techniques could explore the robustness of these results. The increase in
436 annual layer thickness is likely due to a significant increase in mean annual precipitation at the time
437 of original deposition, and warrants further investigation.

438 Ultra-high resolution records are paramount to the assessment and improvement of ice-core
439 chronologies. With respect to the annual layer thickness model and the application of high-
440 resolution trace-element analysis, the results of this study suggest that a combination of
441 glaciological modelling and reliable annual layer thickness observations, derived using ultra-high
442 resolution measurement techniques, would improve the estimation of layer thickness and
443 consequently the age-depth profile of Antarctic ice cores.

444 **Conclusions**

445 LA ICP-MS on ice has the potential to retrieve continuous, seasonal signals from ice core records at
446 depths currently beyond the range of standard laboratory methods. The application of two
447 techniques in high resolution trace element analysis on frozen ice samples from the Berkner Island
448 ice core agree in measurements of annual layer thickness at three depth ranges, providing a detailed
449 snapshot of the Na and Mg seasonal record of the last glacial period. The results of this analysis
450 have been compared with results from a lower-resolution technique applied to parallel sections of
451 ice; trends, depositional peaks in Na and Mg, and absolute values of calibrated concentration in the
452 IC and LA ICP-MS profiles agree – particularly well in the ice originating from the last glacial period.
453 The low sample volume required for LA ICP-MS yields additional information and small-scale
454 variability is resolved in the Holocene profiles. Care and extra assessment of LA ICP-MS profiles
455 should be taken to ensure annual layers are not misidentified during the analysis of ice cores.

456 Assessment of a simple one-dimensional model to estimate the annual layer thicknesses along an ice
457 core confirms that the model is effective at estimating annual layer thicknesses for Holocene and
458 glacial ice on a low resolution. Modelled annual layer thickness for each individual ice section do not
459 compare well with the observed measurements; the model is unable to reconstruct the natural
460 variability on a local scale without a higher resolution stable water isotope profile and better
461 observational data. Optimal annual layer thickness estimates should be constructed using a
462 combination of the glaciological techniques used in the paper, and estimates for compaction rates

463 that are derived using ultra-high resolution analytical techniques such as LA ICP-MS and the discrete
464 sampling technique.

465 *Supplementary Material*

466 In addition to this work, the model explanation and a list of values used in the estimation of the
467 annual layer thickness is included in supplementary material to this paper.

468 *Acknowledgements*

469 An Antarctic Science bursary, a Natural Environment Research Council doctoral training grant, and
470 the US National Science Foundation funded this research. We would also like to thank the editor
471 and the two reviewers, whose comments much improved this manuscript.

472 *Author Contributions*

473 The authors were all involved in the drafting and revisions of the manuscript. Individual input is
474 outlined below:

475 AM prepared all samples of ice for analysis; assisted latest development of discrete sampling
476 technique and contributed to discrete sampling work at BAS; designed and wrote the annual layer
477 thickness model, statistical comparison and wrote the manuscript. GL contributed to the discrete
478 sampling work and analysis by ion chromatography at BAS on Berkner Island; SS conducted the
479 analysis of the ice samples using LA ICP-MS at University of Maine; RT assisted in the ion
480 chromatography analysis of discrete samples; RM assisted design of analysis, model and manuscript;
481 PAM developed the concept and approach of the LA ICP-MS system at the Climate Change Institute,
482 University of Maine; facilitated collaboration between BAS and CCI UMaine; PW assisted design of
483 analysis, model and manuscript.

484

485 *References*

- 486 Arrowsmith, P. 1987. Laser Ablation of Solids for Elemental Analysis by Inductively Coupled Plasma
487 Mass Spectrometry. *Analytical Chemistry*, **59**, 1437-1444.
- 488 Bazin, L., Landais, A., Lemieux-Dudon, B., Toye Mahamadou Kele, H., Veres, D., Parrenin, F.,
489 Martinerie, P., Ritz, C., Capron, E., Lipenkov, V., Loutre, M.-F., Raynaud, D., Vinther, B., Svensson, A.,
490 Rasmussen, S.O., Severi, M., Blunier, T., Leuenberger, M., Fischer, H., Masson-Delmotte, V.,
491 Chappellaz, J., Wolff, E. 2012. An optimized multi-proxy, multi-site Antarctic ice and gas orbital
492 chronology (AICC2012): 120-800ka. *Climate of the Past*, **9**, 1715-1731.
- 493 Bea, F., Montero, P., Stroh, A., Baasner, J. 1996. Microanalysis of minerals by an Excimer UV-LA-ICP-
494 MS system. *Chemical Geology*, **133**, 145-156.
- 495 Björck, S., Walker, M.J.C., Cwynar, L.C., Johnsen, S., Knudsen, K.-L., Lowe, J.J., Wohlfarth, B. and
496 INTIMATE members. 1998. An event stratigraphy for the Last Termination in the North Atlantic
497 region based on the Greenland ice core record: a proposal by the INTIMATE group. *Journal of*
498 *Quaternary Science*, **13**, 283-292.
- 499 Blockley, S.P.E., Lane, C.S., Hardiman, M., Rasmussen, S.O., Seierstad, I.K., Steffensen, J.P., Svensson,
500 A., Lotter, A.F., Turney, C.S.M., Bronk Ramsey, C., INTIMATE members. 2012. Synchronisation of
501 palaeoenvironmental records over the last 60,000 years, and an extended INTIMATE event
502 stratigraphy to 48,000 b2k. *Quaternary Science Reviews*, **36**, 2-10.
- 503 Broecker, W.S. 1998. Paleocean circulation during the last deglaciation: a bipolar seesaw?
504 *Palaeoceanography*, **13**, 119-121.
- 505 Dansgaard, W., 1953. The abundance of ¹⁸O in atmospheric water and water vapour. *Tellus*, **5**, 461-
506 469.
- 507 Dansgaard, W., 1964. Stable Isotopes in Precipitation. *Tellus*, **16**, 436-468.

508 Dansgaard et al., 1993. Evidence for general instability of past climate from a 250-kyr ice-core
509 record. *Nature*, **364**, 218-220.

510 EPICA Community Members, 2006. One-to-one coupling of glacial climate variability in Greenland
511 and Antarctica. *Nature*, **444**, doi: 10.1038/nature05301.

512 Gillet-Chaulet, F., Hindmarsh, R.C.A., Corr, H.F.J., King, E.C., Jenkins, A. 2011. *In-situ* quantification of
513 ice rheology and direct measurement of the Raymond Effect at Summit, Greenland using a phase-
514 sensitive radar. *Geophysical Research Letters*, **38**, doi: 10.1029/2011GL049843

515 Haines, S.A., Mayewski, P.A., Kurbatov, A.V., Maasch, K.A., Sneed, S.B., Spaulding, N.E., Dixon, D.A.,
516 Bohleber, P.D. 2016. Ultra-high resolution snapshots of three multi-decadal periods in an Antarctic
517 ice core. *Journal of Glaciology*, **62**, doi: 10.1017/jog.2016.5

518 Hindmarsh, R.C.A., King, E.C., Mulvaney, R., Corr, H.F.J., Hiess, G., Gillet-Chaulet, F. 2011. Flow at ice-
519 divide triple junctions: 2. Three-dimensional views of isochrone architecture from ice-penetrating
520 radar surveys. *Journal of Geophysical Research*, **116**, doi: 10.1029/2009JF001622

521 Jouzel, J., Barkov, N.I., Barnola, J.-M., Genthon, C., Korotkevitch, Y.S., Kotlyakov, V.M., Legrand, M.,
522 Lorius, C., Petit, J.-P., Petrov, V.N., Raisbeck, G., Raynaud, D., Ritz, C., Yiou, F. 1989. Global change
523 over the last climatic cycle from the Vostok ice core record (Antarctica). *Quaternary International*, **2**,
524 15-24.

525 Kawamura, K., Parrenin, F., Lisiecki, L., Uemura, R., Vimeux, F., Severinghaus, J.P., Hutterli, M.A.,
526 Nakazawa, T., Aoki, S., Jouzel, J., Raymo, M.E., Matsumoto, K., Nakata, H., Motoyama, H., Fujita, S.,
527 Goto-Azuma, K., Fujii, Y., Watanabe, O. 2007. Northern hemisphere forcing of climatic cycles in
528 Antarctica over the past 360,000 years. *Nature*, **448**, doi: 10.1038/nature06015.

529 Kingslake, J., Hindmarsh, R.C.A., Aðalgeirsdóttir, G., Conway, H., Corr, H.F.J., Gillet-Chaulet, F.,
530 Martin, C., King, E.C., Mulvaney, R., Pritchard, H.D. 2014. Full-depth englacial vertical ice sheet

531 velocities measured using phase-sensitive radar. *Journal of Geophysical Research: Earth Surface*,
532 **119**, doi: 10.1002/2014JF003275.

533 Lemieux-Dudon, B., Blayo, E., Petit, J.-R., Waelbroeck, C., Svensson, A., Ritz, C., Barnola, J.-M.,
534 Narcisi, B.M., Parrenin, F. 2010. Consistent dating for Antarctic and Greenland ice cores. *Quaternary*
535 *Science Reviews*, **29**, 8-20.

536 Lliboutry, L. and Duval, P. 1985. Various isotropic and anisotropic ices found in glaciers and polar ice
537 caps and their corresponding rheologies. *Annales Geophysicae*, **3**, 207-224.

538 Louergue, L., Schilt, A., Spahni, R., Masson-Delmotte, V., Blunier, T., Lemieux, B., Barnola, J.-M.,
539 Raynaud, D., Stocker, T.F., Chappellaz, J. 2008. Orbital and millennial-scale features of atmospheric
540 CH₄ over the past 800,000 years. *Nature*, **453**, 383-386.

541 Luthi, D., Le Floch, M., Bereiter, B., Blunier, T., Barnola, J.-M., Siegenthaler, U., Raynaud, D., Jouzel, J.,
542 Fischer, H., Kawamura, K., Stocker, T.F. 2008. High-resolution carbon dioxide concentration record
543 650,000-800,000 years before present. *Nature*, **453**, 379-382.

544 Mani, F.S. 2010. *Measurements of $\delta^{15}N$ of nitrogen gas and composition of trace gases in air from*
545 *firn and ice cores*. PhD Thesis, University of East Anglia, UK.

546 Mayewski, P.A., Sneed, S.B., Birkel, S.D., Kurbatov, A.V., Maasch, K.A. 2014. Holocene warming
547 marked by abrupt onset of longer summers and reduced storm frequency around Greenland. *Journal*
548 *of Quaternary Science*, **29**, 99-104.

549 Müller, W., Shelley, J.M.G., Rasmussen, S.O. 2011. Direct chemical analysis of frozen ice cores by UV
550 laser ablation ICPMS. *Journal Analytical Atmospheric Spectrometry*, **26**, 2391-2395.

551 Mulvaney, R., Alemany, O., Possenti, P. 2007. The Berkner Island (Antarctica) ice-core drilling
552 project. *Annals of Glaciology*, **47**, 115-124.

553 Parrenin, F., & Hindmarsh, R. 2007. Influence of a non-uniform velocity field on isochrone geometry
554 along a steady flowline of an ice sheet. *Journal of Glaciology*, **53**, 612-622.

555 Parrenin, F., Dreyfus, G., Durand, G., Fujita, S., Gagliardini, O., Gillet, F., Jouzel, J., Kawamura, K.,
556 Lhomme, N., Masson-Delmotte, V., Ritz, C., Schwander, J., Shoji, H., Uemura, R., Watanabe, O.,
557 Yoshida, N., 2007. 1-D-ice flow modelling at EPICA Dome C and Dome Fuji, East Antarctica. *Climate of*
558 *the Past*, **3**, 243-259.

559 Parrenin, F., Bazin, L., Capron, E., Landais, A., Lemieux-Dudon, B., Masson-Delmotte, V. 2015.
560 IceChrono1: a probabilistic model to compute a common and optimal chronology for several ice
561 cores. *Geoscientific Model Development*, **8**, 1473-1492.

562 Reinhardt, H., Kriews, M., Miller, H., Schrems, O., Lüdke, C., Hoffman, E., Skole, J. 2001. Laser
563 ablation inductively coupled plasma mass spectrometry: a new tool for trace element analysis in ice
564 cores. *Fresenius Journal of Analytical Chemistry*, **370**, 629-636.

565 Rothlisberger, R., Bigler, M., Hutterli, M., Sommer, S., Stauffer, B. 2000. Technique for continuous
566 high-resolution analysis of trace substances in firn and ice cores. *Environmental Science &*
567 *Technology*, **34 (2)**, pp. 338-342.

568 Ruddiman, W.F. and Raymo, M.E. 2006. A methane-based time scale for Vostok ice. *Quaternary*
569 *Science Reviews*, **22**, 141-155.

570 Severinghaus, J. 2009. Southern see-saw seen. *Nature*, **457**, 1093-1094.

571 Shackleton, N.J. The 100,000 year ice-age cycle identified and found to lag temperature, carbon
572 dioxide, and orbital eccentricity. *Science*, **289**, 1897-1902.

573 Sigg, A., Fuhrer, K., Anklin, M., Staffelbach, T., Zurmühle, D. 1994. A continuous analysis technique for
574 trace species in ice cores. *Environmental Science & Technology*, **28(2)**, 204-209.

575 Sneed, S.B., Mayewski, P.A., Sayre, W.G., Handley, M.J., Kurbatov, A.V., Taylor, K.C., Bohleber, P.,
576 Wagenbach, D., Erhardt, T., Spaulding, N.E. 2015. New LA-ICP-MS cryocell and calibration technique
577 for sub-millimeter analysis of ice cores. *Journal of Glaciology*, **226**, 233-242.

578 Sommer, S., Appenzeller, C., Röthlisberger, R., Hutterli, M.A., Stauffer, B., Wagenbach, D., Oerter, H.,
579 Wilhelms, F., Miller, H., Mulvaney, R. 2000. Glacio-chemical study spanning the past 2 kyr on three
580 ice cores from Dronning Maud Land, Antarctica: 1. Annually resolved accumulation rates. *Journal of*
581 *Geophysical Research: Atmospheres*, **105**, 29411-29421.

582 Tarantola, A. 1987. Inverse problem theory: Methods for data fitting and model parameter
583 estimation. *Elsevier Science*, New York.

584 Thomas, E.R., Wolff, E.W., Mulvaney, R., Johnsen, S.J., Steffensen, J.P., Arrowsmith, C. 2009.
585 Anatomy of a Dansgaard-Oeschger warming transition: high resolution analysis of the North
586 Greenland Ice Core Project ice core. *Journal of Geophysical Research*, **114**, DOI:
587 10.1029/2008JD011215.

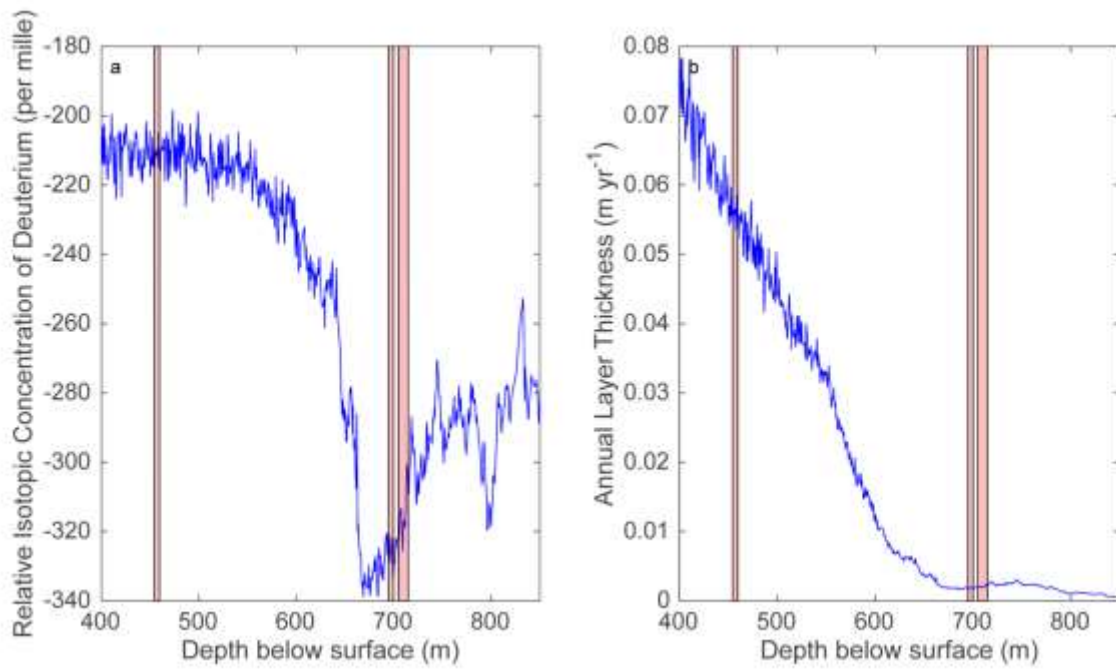
588 Wagenbach, D., Graf, W., Minikin, A., Trefzer, U., Kippstuhl, J., Oerter, H., Blindow, N. 1994.
589 Reconnaissance of chemical and isotopic firn properties on top of Berkner Island, Antarctica. *Annals*
590 *of Glaciology*, **20**, 307-312.

591 WAIS Divide Project Members, 2015. Precise inter-polar phasing of abrupt climate change during the
592 last ice age. *Nature*, **520**, 661-665.

593 Weertman, J. 1973. The Creep of Ice. In: Whalley, E., Jones, S.J., Gold, L.W. (Eds.). *Physics and*
594 *chemistry of ice: papers presented at the Symposium on the Physics and Chemistry of Ice, held in*
595 *Ottawa, Canada, 14-18 August 1972*, Ottawa, Royal Society of Canada, 320-337.

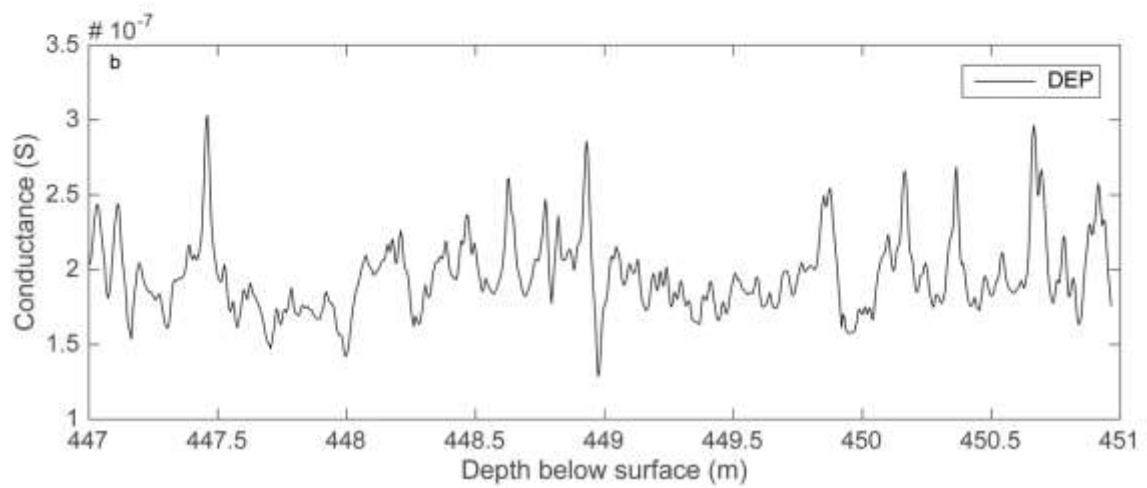
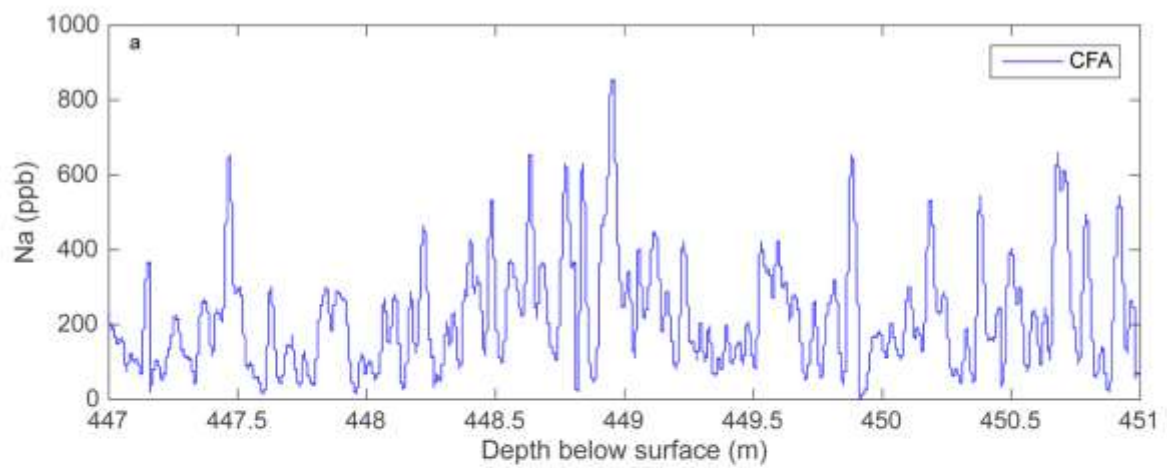
596

597



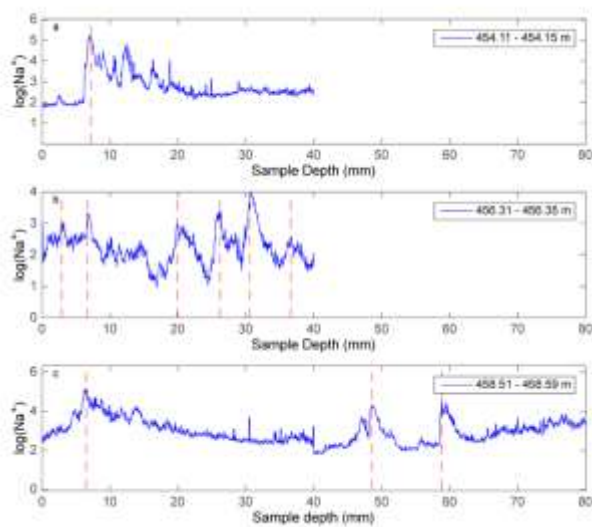
599

600 Figure 1 (Left to right): Berkner Island ice core sampled sections of ice (pink bands) across the
601 isotopic (left) and modelled annual layer thickness profiles (right).



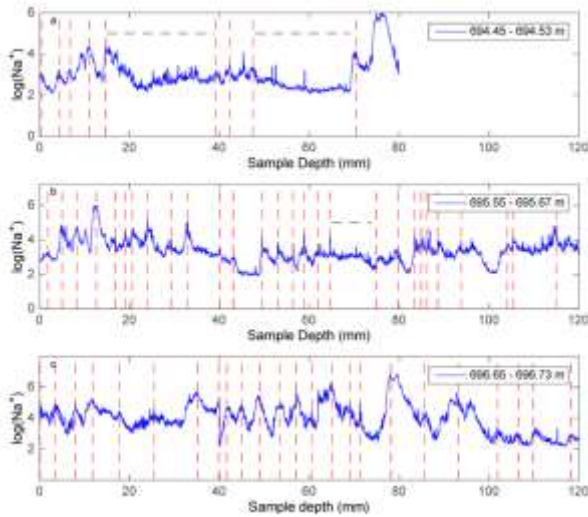
602

603 Figure 2 (Top to bottom): Four-metre section analysed by CFA and DEP. Top: CFA Na; bottom: DEP.

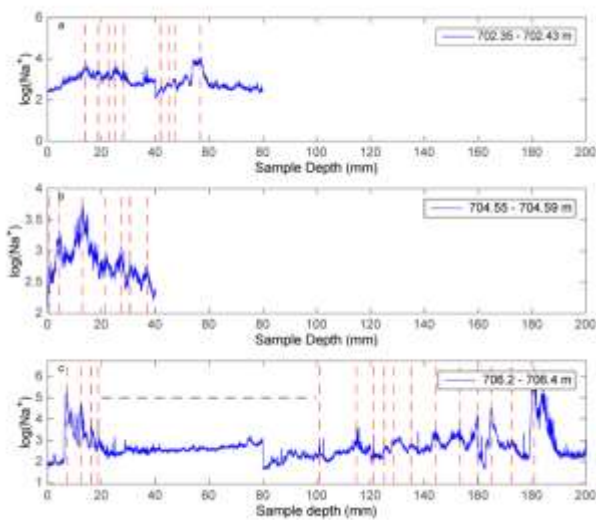


604

605 Figure 3a – c: LA ICP-MS profiles for three sections of sample from 454 – 459 m; semi logarithmic
606 plots show the $\log(\text{Na}^+)$ on a common depth scale with red dashed lines delineating a seasonal peak.

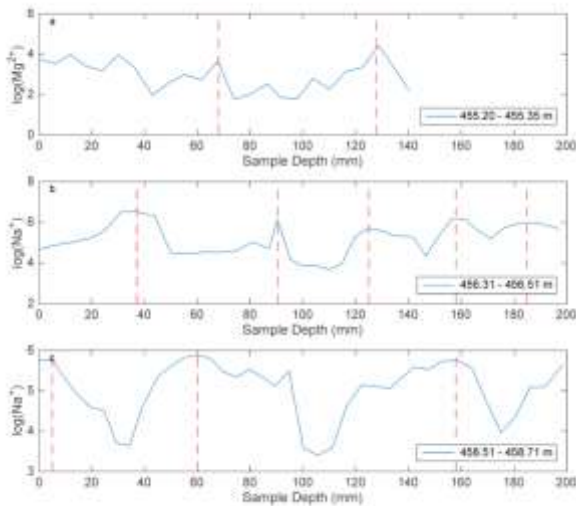


607
608 Figure 4a – c: LA ICP-MS profiles for three sections of ice from 694-697 m; semi logarithmic plots
609 show the $\log(\text{Na}^+)$ on a common depth scale with red dashed lines delineating a seasonal peak.
610 Black dashed lines indicate where no annual layers are discernible.

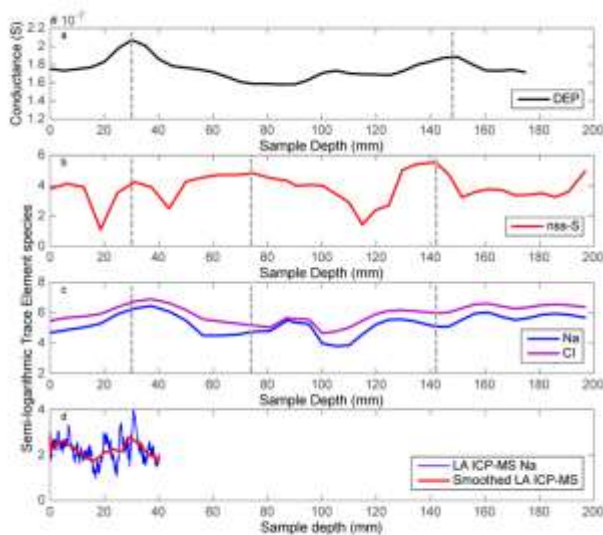


611

612 Figure 5a – c: LA ICP-MS profiles for three sections of ice from 702 - 707 m; semi logarithmic plots
 613 show the log(Na+) on a common depth scale with red dashed lines delineating a seasonal peak.
 614 Black dashed lines indicate where no annual layers are discernible.

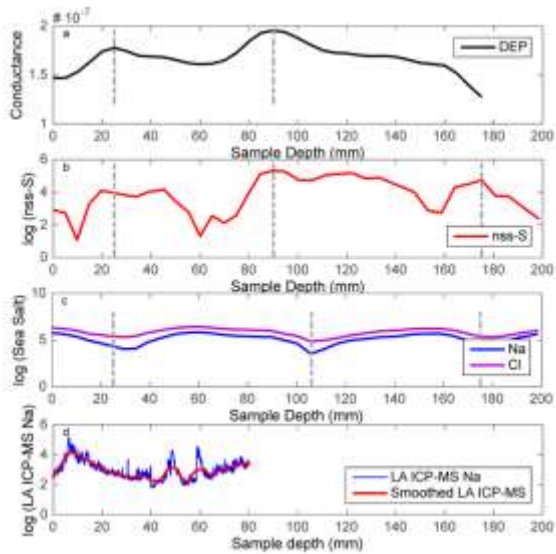


615
 616 Figure 6 (Top to bottom): Three sections of ice originating from 455 – 459 m analysed by ion
 617 chromatography and displayed as semi logarithmic plots of element concentration with red dashed
 618 lines indicating annual peaks.



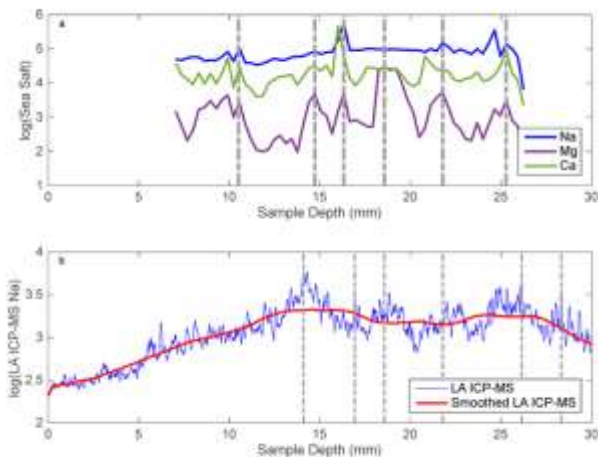
619
 620 Figure 7: Comparison of parallel sections of ice from 456.31 m – 456.51 m from top to bottom: the
 621 DEP data; nss-S profile analysed by discrete sampling; sodium and chloride profiles analysed by

622 discrete sampling; ice analysed by LA ICP-MS with the profile smoothed to the same resolution used
623 in the discrete sampling technique, with annual layers indicated by grey lines.



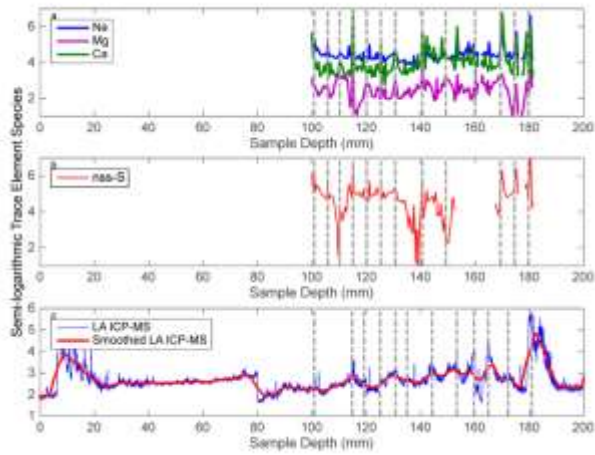
624

625 Figure 8a: Comparison of parallel sections of ice from 458.51 – 458.71 m from top to bottom: the
626 DEP data; nss-S profile analysed by discrete sampling (red); sodium and chloride profiles analysed by
627 discrete sampling; ice analysed by LA ICP-MS with the profile smoothed to the same resolution used
628 in the discrete sampling technique (red), with annual layers indicated by grey lines.



629

630 Figure 9: Comparison of parallel sections of ice from 703.2 - 703.22 m from top to bottom: ice
631 analysed by discrete sampling technique; ice analysed via LA ICP-MS with a smoothed profile (red).
632 Black dashed lines indicate where no annual layers are discernible.



633

634

Figure 10: Comparison of parallel sections of ice from 706.3 - 706.38 m from top to bottom: ice

635

analysed by discrete sampling technique; the nss-S profile from the discrete sampling technique; ice

636

analysed via LA ICP-MS with a smoothed profile (red). Black dashed lines indicate where no annual

637

layers are discernible.

638

639 Table I: Annual layer thickness determined as the mean thickness value of all layers identified in each
 640 analysed section, and the standard deviation of each set of annual layers. Modelled annual layer
 641 thickness given with model error attached. For depths that have not been analysed by a particular
 642 technique, the table reads "N/A". The estimated age for each sample depth is presented, as
 643 estimated by the age-depth model.

Depth Analysed (m)	LA ICP-MS +/- std dev (mm)	Discrete Sampling +/- std dev (mm)	CFA +/- std dev (mm)	Model +/- error (mm)	Estimated age (ka BP)
447-451	N/A	N/A	57.0 ± 8.8	57.0 ± 1.9	5.0
454	Variable	57.0 ± 10.0	N/A	51.2 ± 1.9	5.5
456	6.7 ± 0.6	55.0 ± 1.3	N/A	49.8 ± 1.9	5.6
458	26.1 ± 2.3	70.0 ± 2.8	N/A	49.4 ± 1.9	5.6
694	2.9 ± 0.1	N/A	N/A	3.0 ± 0.2	27.1
695	3.6 ± 0.1	N/A	N/A	3.1 ± 0.2	27.4
696	4.0 ± 0.2	N/A	N/A	3.1 ± 0.2	27.7
702	3.1 ± 0.1	2.6 ± 0.1	N/A	2.8 ± 0.1	29.7
704	6.1 ± 0.2	N/A	N/A	2.9 ± 0.1	30.4
706	5.1 ± 0.2	6.0 ± 2.3	N/A	2.8 ± 0.1	31.1

644

645